Unusual Appearances of Uterine Leiomyomas: MR Imaging Findings and Their Histopathologic Backgrounds[1]

Hiroyuki Ueda, MD • Kaori Togashi, MD • Ikuo Konishi, MD
Milliam L. Kataoka, MD • Takashi Koyama, MD • Toshitaka Fujiwara, MD • Hisataka Kobayashi, MD • Shingo Fujii, MD
Junji Konishi, MD

Typical appearances of uterine leiomyoma at magnetic resonance (MR) imaging are well established, and diagnosis is usually easy. However, cases that are extremely difficult to differentiate from other conditions are occasionally encountered. To understand the wide spectrum of MR imaging findings, such unusual appearances can be classified into three categories: degeneration and other histopathologic findings, specific types of unusual leiomyomas, and unusual growth patterns. The common types of degeneration are hyaline (>60% of cases), cystic (~4%), myxoid, and red. Edema is not a phenomenon of degeneration but is a common histopathologic finding (~50% of cases). Hemorrhage, necrosis, and calcification (~4% of cases) may also be observed. Specific types of unusual leiomyomas include lipoleiomyoma and myxoid leiomyoma, which may have MR imaging features characteristic enough to allow differentiation from other gynecologic and nongynecologic diseases. Intravenous leiomyomatosis, metastasizing leiomyoma, diffuse leiomyomatosis, and peritoneal disseminated leiomyomatosis represent unusual growth patterns; other unusual growth patterns are retroperitoneal growth, parasitic growth, and the pattern that may occur in cervical leiomyoma. Because leiomyomas are the most common gynecologic tumors and are exclusively benign, it is important to be familiar with the variety of MR imaging appearances of uterine leiomyomas to distinguish them from other significant diseases.

Index terms: Leiomyoma, 854.315 • Uterine neoplasms, diagnosis, 854.315 • Uterine neoplasms, MR, 854.1214, 854.315

RadioGraphics 1999; 19:S131–S145

[1]From the Departments of Nuclear Medicine and Diagnostic Imaging (H.U., M.L.K., T.K., T.F., J.K.), Diagnostic and Interventional Imageology (K.T., H.K.), and Gynecology and Obstetrics (I.K., S.F.), Graduate School of Medicine, Kyoto University, 54 Shogoin Kawahara-cho, Sakyo-ku, Kyoto 606-8507, Japan. Recipient of a Certificate of Merit award for a scientific exhibit at the 1998 RSNA scientific assembly. Received February 2, 1999; revision requested March 3; final revision received April 26; accepted April 29. **Address reprint requests to** K.T.

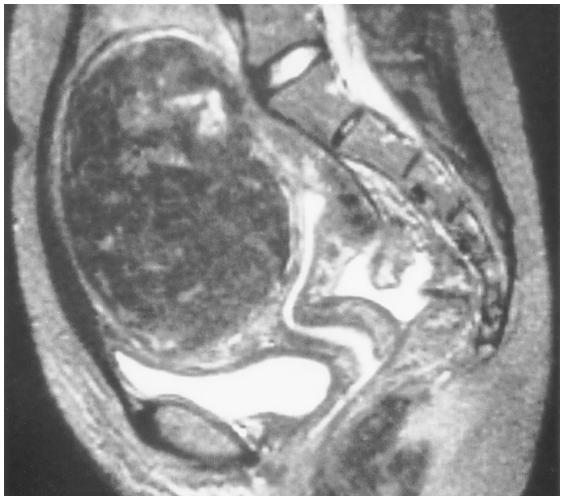

a.

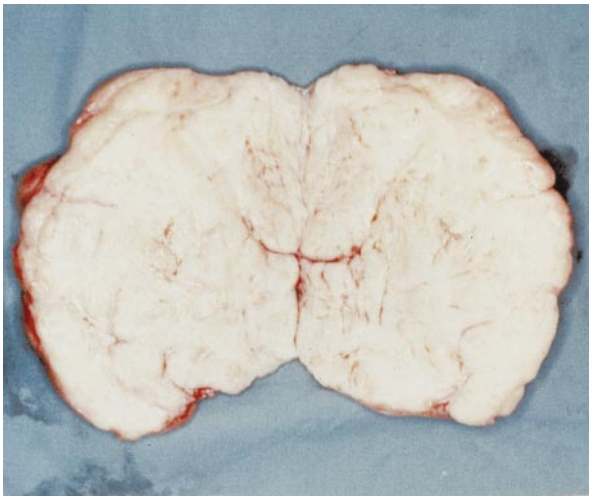

b.

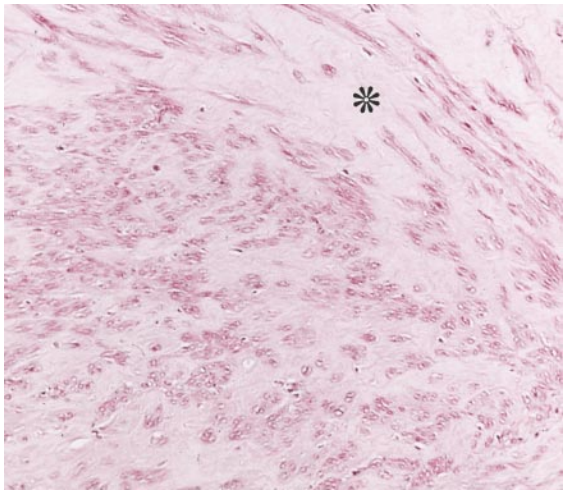

c.

Figure 1. Typical leiomyoma in a 37-year-old woman. **(a)** Sagittal spin-echo T2-weighted MR image (2,000/70 [repetition time msec/echo time msec]) shows a well-demarcated mass of distinct low signal intensity with a speckled appearance. **(b)** Photograph of the cut surface of the resected lesion shows a white mass with a speckled appearance. **(c)** Photomicrograph (original magnification, ×100; hematoxylin-eosin stain) shows hyaline degeneration throughout the lesion (*).

■ INTRODUCTION

Leiomyomas are by far the most common uterine tumors and the most common gynecologic tumors. Extremely prevalent, they occur in more than 20% of women older than 30 years (1,2). Their typical appearances at magnetic resonance (MR) imaging have been well established (3,4). However, leiomyomas vary widely in appearance and may be confused with other gynecologic malignancies. Precise knowledge of the histopathologic backgrounds of degeneration and the clinical course helps us accurately diagnose leiomyomas with unusual appearances.

In this article, the spectrum of MR imaging findings in uterine leiomyoma is presented with emphasis on the findings that help characterize the lesion. Unusual appearances are discussed from three points of view: MR imaging–histopathologic correlation, specific types of unusual leiomyomas, and unusual growth patterns.

■ MR IMAGING–HISTOPATHOLOGIC CORRELATION

Leiomyomas typically demonstrate distinct low signal intensity relative to that of the myometrium on T2-weighted images and intermediate signal intensity on T1-weighted images. These characteristic signal intensities are attributed to extensive hyalinization, which occurs in more than 60% of uterine leiomyomas (1,5,6). However, leiomyomas can demonstrate various histopathologic patterns of degeneration, some

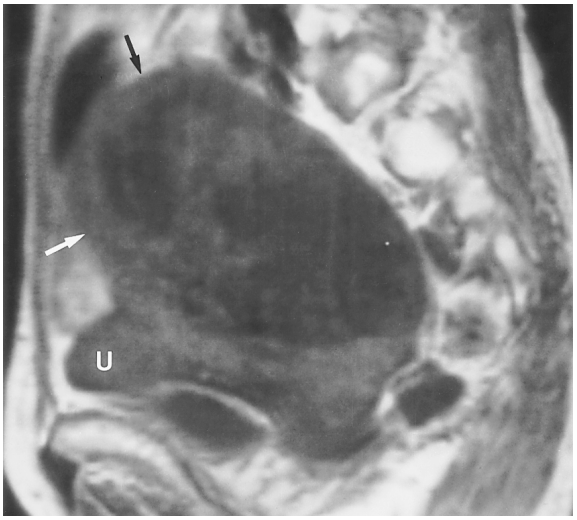

a.

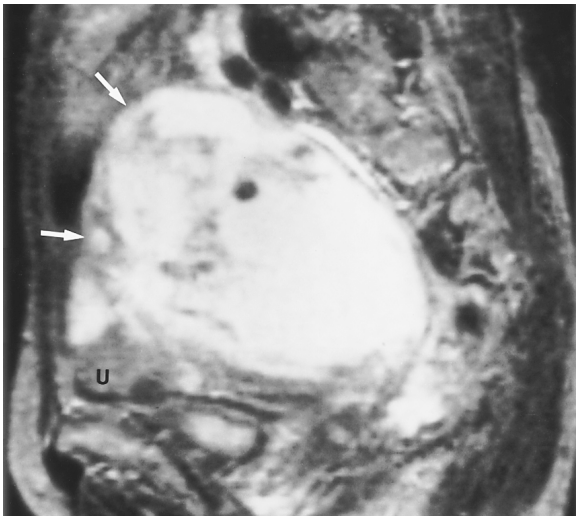

b.

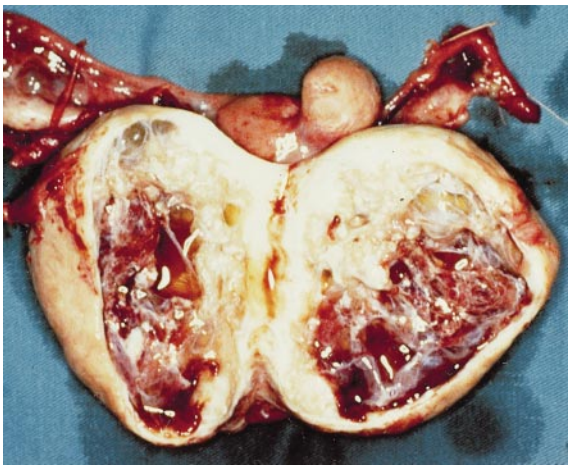

c.

Figure 2. Subserosal leiomyoma with extensive cystic degeneration in a 61-year-old woman. **(a, b)** Sagittal spin-echo T1-weighted (600/25) **(a)** and T2-weighted (2,000/70) **(b)** MR images show a mass posterior to the uterus (*U*) (arrows). The signal intensity of the mass corresponds to fluid mixed with thin, interlacing tissue of intermediate signal intensity on both images. **(c)** Photograph of the cut surface of the resected lesion shows an almost entirely cystic mass with scanty solid tissue. (Reprinted, with permission, from reference 4.)

of which alter the MR imaging appearance. The common types of degeneration are hyaline, cystic, myxoid, and red. Edema is not a phenomenon of degeneration but is a common histopathologic finding, present in about 50% of leiomyomas (1). Hemorrhage, necrosis, and calcification may also be observed. In this section, a wide variety of MR imaging findings in uterine leiomyoma and their histopathologic backgrounds are described.

• Degeneration

The most common type of degeneration is focal or generalized hyalinization. Hyalinization occurs in more than 60% of leiomyomas and is usually extensive (1,5,6). At the microscopic level, hyalinization begins in the stromal component that separates the smooth muscle cells and then progresses to extensive replacement of the smooth muscle cells (2). The typical MR imaging feature of leiomyoma—distinct low signal intensity on T2-weighted images—is due to extensive hyalinization (7,8) (Fig 1).

Edema may change into various degrees of collagen deposition and cystic degeneration (6). Cystic degeneration may be considered an extreme sequela of edema and is observed in about 4% of leiomyomas (1). Large or small cystic spaces develop in the edematous, acellular center (1,5,6). The cystic spaces appear as round, well-demarcated areas with the signal intensity characteristic of fluid: low on T1-weighted images and high on T2-weighted images with no enhancement (Fig 2).

Myxoid degeneration appears as soft mucoid areas, sometimes with cystic change (2). Leiomyomas with this type of degeneration are basically benign and appear as cystic masses filled with gelatinous material (Fig 3). However,

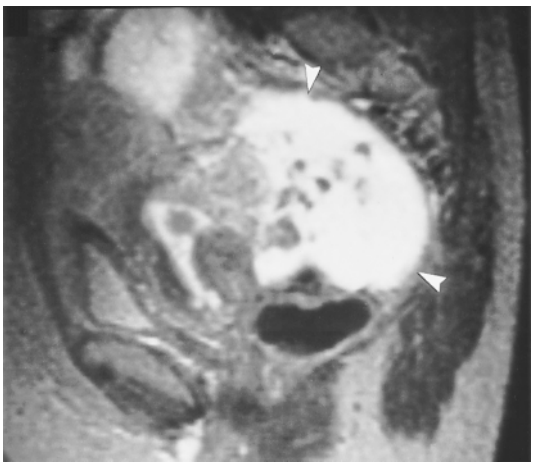

a.

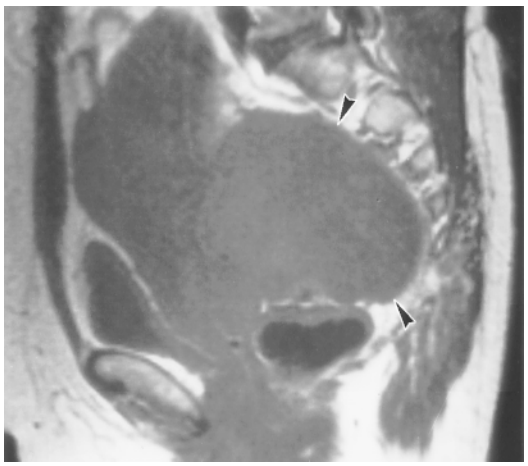

b.

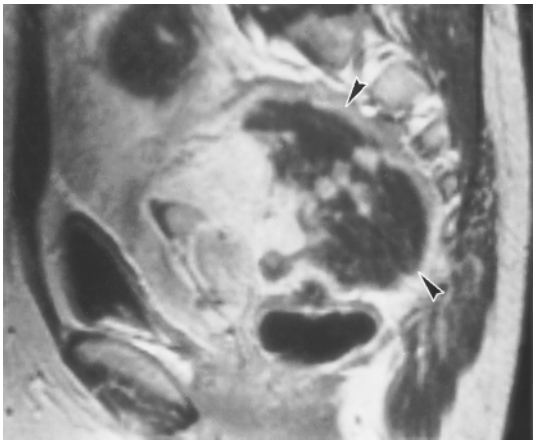

c.

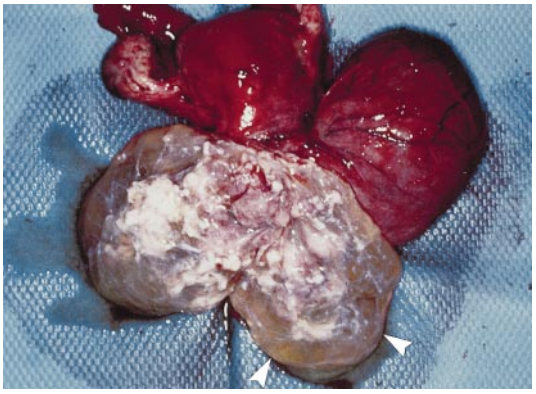

d.

Figure 3. Leiomyoma with myxoid degeneration in a 55-year-old woman. **(a–c)** Sagittal spin-echo T2-weighted (2,000/70) **(a)**, T1-weighted (600/20) **(b)**, and gadolinium-enhanced T1-weighted (600/20) **(c)** MR images show a mass arising from the uterine cervix that has mixed solid and cystic components. Myxoid material (arrowheads) demonstrates high signal intensity on the T2-weighted image **(a)**, low signal intensity on the T1-weighted image **(b)**, and no enhancement on the gadolinium-enhanced image **(c)**. Viable tissue has relatively low signal intensity on the T2-weighted image **(a)** and is well enhanced on the gadolinium-enhanced image **(c)**. **(d)** Photograph of the cut surface of the resected lesion shows a cystic mass filled with gelatinous material (arrowheads).

myxoid degeneration is important because it may also be seen in leiomyosarcomas and other malignant tumors (2). A tumor with extensive myxoid change may be diagnosed as myxoid leiomyoma, which is discussed later in this article (1,2).

Red or carneous degeneration involves massive hemorrhagic infarction of a leiomyoma due to obstruction of drainage veins at the periphery of the lesion. Such degeneration is a kind of extensive coagulative necrosis that involves the entire lesion. This condition occurs most often during pregnancy and is also associated with use of oral contraceptives (1,5,6).

Unlike other types of degeneration, red degeneration usually causes systemic symptoms. Findings at MR imaging reflect the pathogenesis of this condition well and contribute to an accurate diagnosis (9). The peripheral rim, which has distinct low signal intensity on T2-weighted images and high signal intensity on T1-weighted images, corresponds to the obstructed veins at the periphery of the mass (Fig 4). The entire lesion shows no enhancement, which indicates complete interruption of blood flow.

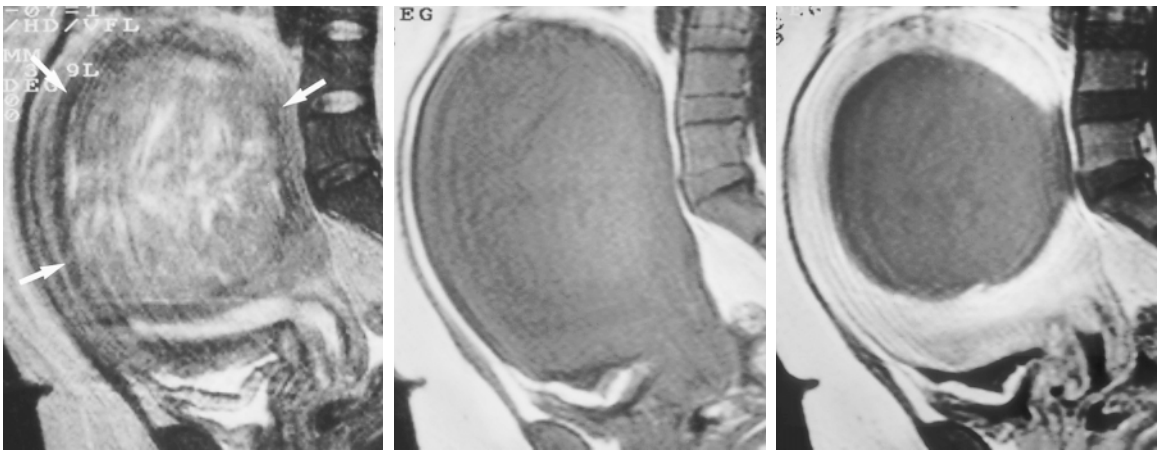

a. b. c.

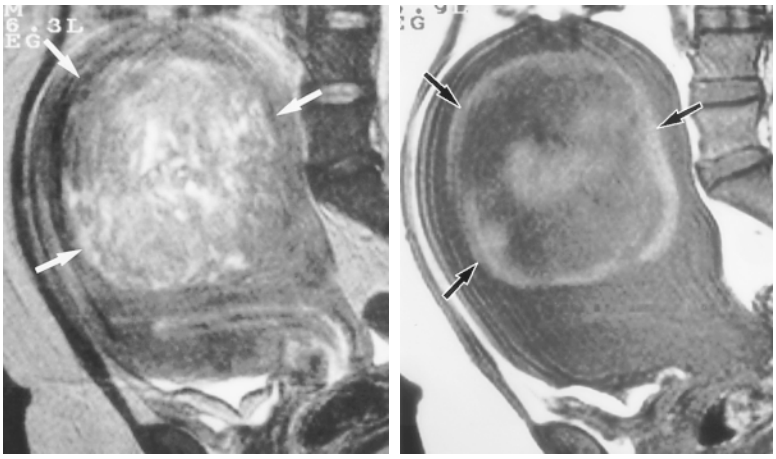

d. e.

f.

g.

Figure 4. Red degeneration in a 44-year-old woman with sudden onset of abdominal pain. **(a)** Sagittal fast spin-echo T2-weighted MR image (5,000/100) obtained several hours after onset shows a thick rim of distinct low signal intensity that corresponds to acute hemorrhage (arrows). **(b)** Sagittal spin-echo T1-weighted MR image (600/13) obtained several hours after onset shows no significant findings. **(c)** Sagittal gadolinium-enhanced spin-echo T1-weighted MR image (600/13) obtained several hours after onset shows complete absence of enhancement, a finding that indicates infarction. **(d, e)** Sagittal fast spin-echo T2-weighted (5,500/100) **(d)** and spin-echo T1-weighted (600/13) **(e)** MR images obtained 1 week later show a thick rim of distinct low signal intensity on the T2-weighted image (arrows in **d**) and high signal intensity on the T1-weighted image (arrows in **e**) that corresponds to subacute hemorrhage. **(f,g)** Permission to reprint these figures electronically was denied by the publisher. See print version.

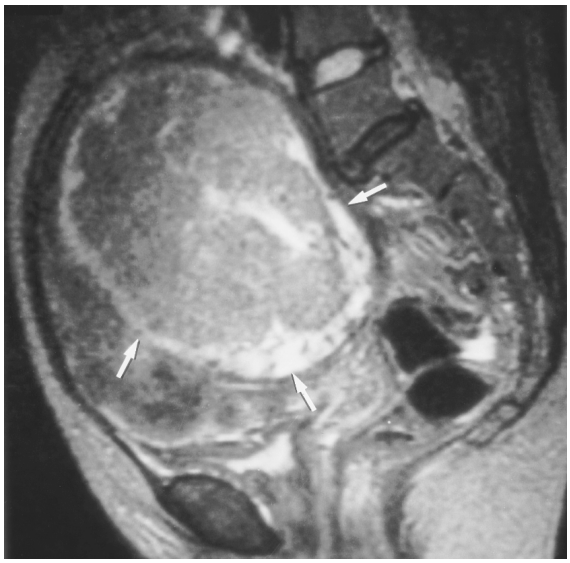

a.

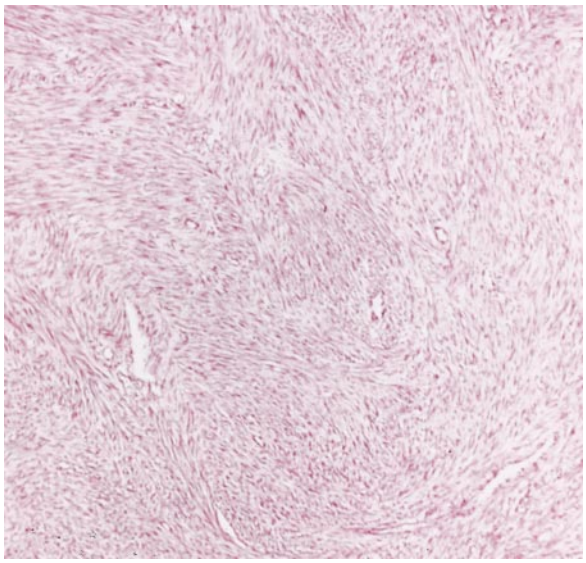

b.

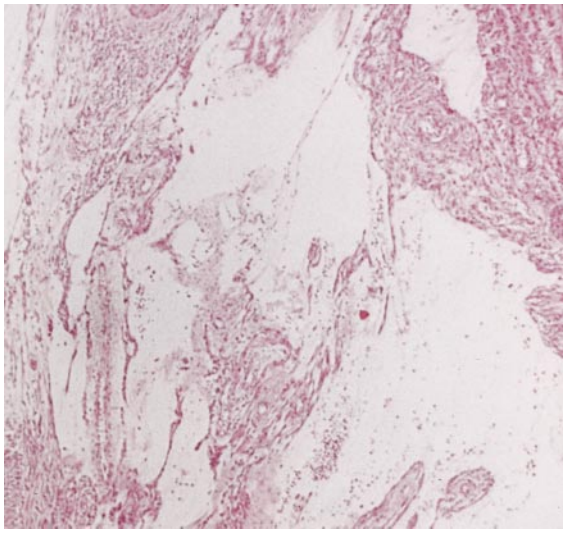

c.

Figure 5. Leiomyoma consisting of a cellular component and peripheral edema in a 45-year-old woman. **(a)** Sagittal T2-weighted spin-echo MR image (2,000/70) shows a mass of intermediate signal intensity with a high-signal-intensity periphery (arrows). **(b, c)** Photomicrographs (original magnification, ×20; hematoxylin-eosin stain) show tightly packed smooth muscle cells in the central zone **(b)** and prominent edema with large vessels at the periphery **(c)**.

• Edema

Edema is not necessarily secondary to degeneration. Fluid accumulates for multiple reasons, and edema is a common histopathologic finding, observed in about 50% of leiomyomas. The presence of edema strongly affects the signal intensity of leiomyomas and may antedate hyalinization and cystic degeneration (1,5,6). The edema is scattered throughout the lesion in a speckled pattern but is frequently prominent at the periphery (10) (Fig 5). It is important to consider peripheral lymphedema in the diagnosis of leiomyoma, whereas central necrosis is a common finding in ovarian tumors. With extensive edema, the entire lesion has high signal intensity on T2-weighted images and demonstrates marked enhancement (11) (Fig 6). The high signal intensity on T2-weighted images is attributed to the accumulation of fluid, and the prominent enhancement is explained by retention of contrast material within the abundant interstitial spaces (11). At microscopy, fluid is seen in the stroma of the leiomyoma, often in association with collagen.

• Hemorrhage and Necrosis

Hemorrhage and necrosis (other than red degeneration) are not common but may be observed in leiomyomas. The recent trend in histopathologic diagnosis of leiomyosarcoma is to consider the presence of coagulative necrosis and hemorrhage (12). Thus, attention should be paid to hemorrhage and necrosis as clues in the diagnosis of sarcoma. However, red degeneration is an exception to this rule; furthermore, hemorrhage and necrosis do occur in some leiomyomas (Fig 7) (1,5,6,13). The damaged smooth muscle will eventually be replaced by firm collagenous tissue (1).

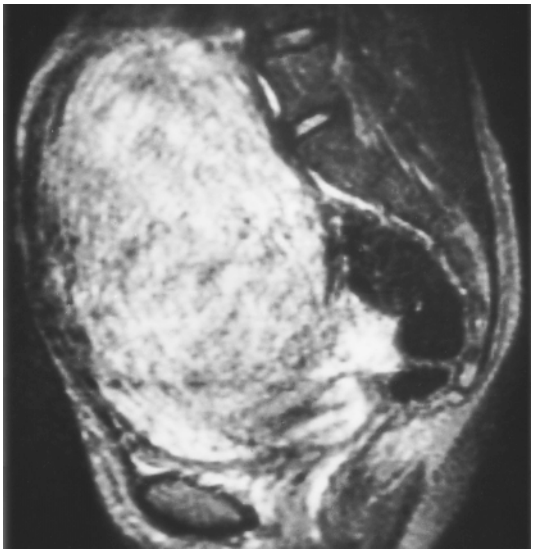

a.

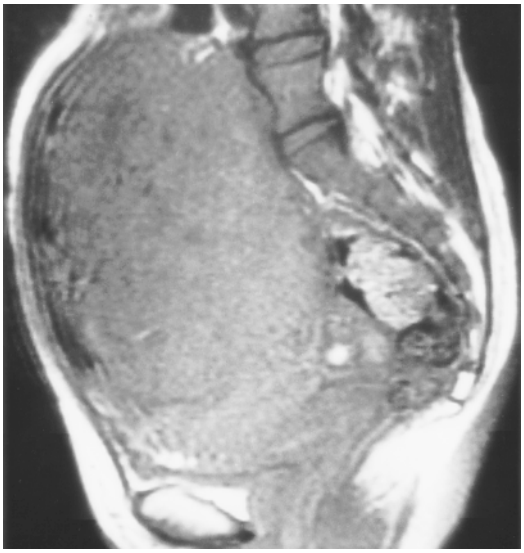

b.

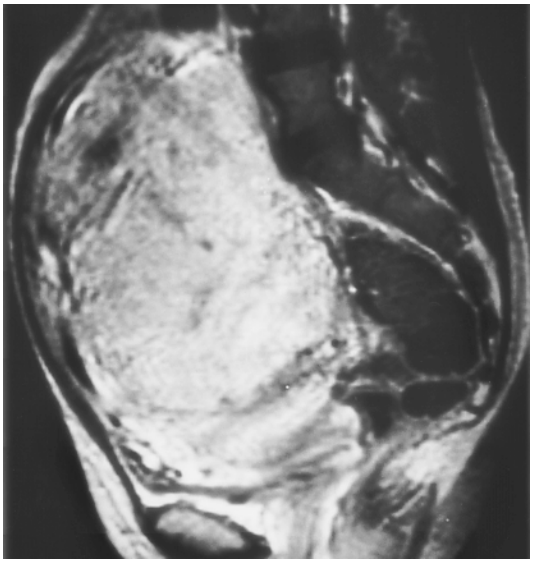

c.

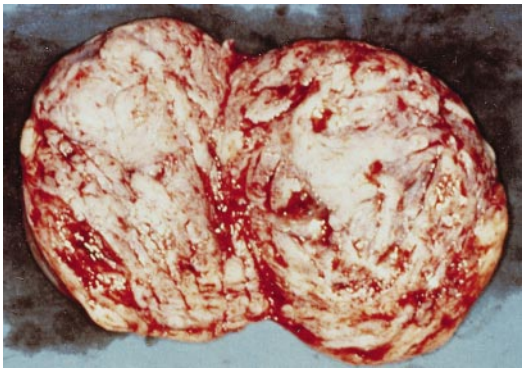

d.

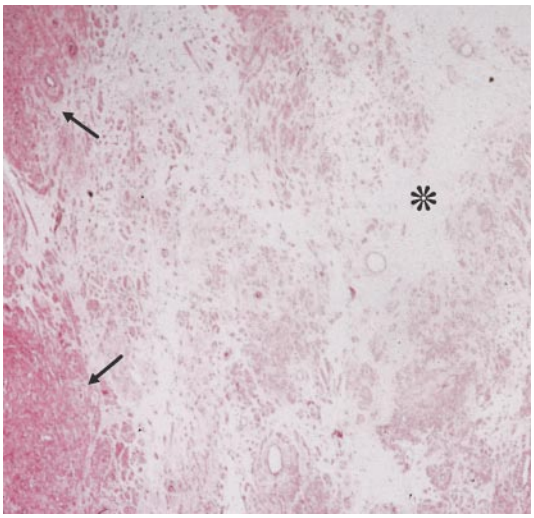

e.

Figure 6. Leiomyoma with extensive edema in a 25-year-old woman. **(a)** Sagittal spin-echo T2-weighted MR image (2,000/70) shows a large mass of high signal intensity with scattered foci of low signal intensity arising from the uterus. **(b, c)** Sagittal nonenhanced **(b)** and gadolinium-enhanced **(c)** spin-echo T1-weighted MR images (600/20) show prominent enhancement of the entire mass except for small foci of cystic changes. **(d)** Photograph of the cut surface of the resected lesion shows a soft, pink mass. **(e)** Photomicrograph (original magnification, ×20; hematoxylin-eosin stain) shows sparse smooth muscle cells (arrows) scattered within an area of extensive edema (*). No hyalin is present.

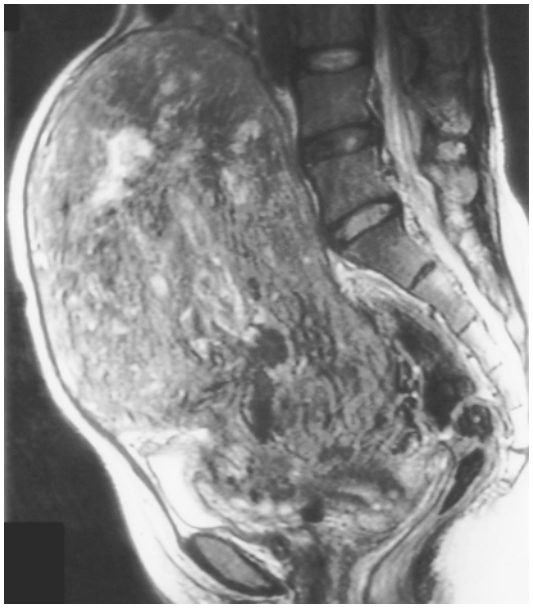

a.

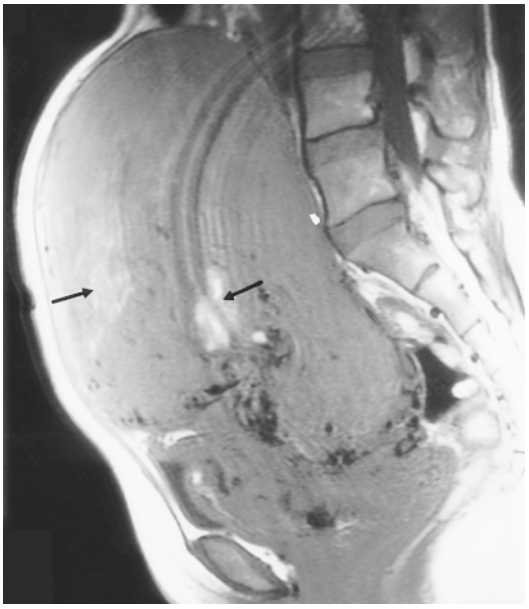

b.

Figure 7. Cellular leiomyoma with coagulative necrosis in a 44-year-old woman. **(a)** Sagittal fast spin-echo T2-weighted MR image (6,000/126) shows a mass of relatively low signal intensity. Hemorrhage and necrosis are not obvious. **(b, c)** Sagittal nonenhanced **(b)** and gadolinium-enhanced **(c)** spin-echo T1-weighted MR images (600/9) show irregular areas of necrosis (arrows). The necrotic areas have high signal intensity on the T1-weighted image **(b)** and demonstrate no enhancement on the gadolinium-enhanced image **(c)**. **(d)** Photograph of the cut surface of the resected lesion shows a fleshy mass with focal hemorrhage (arrows).

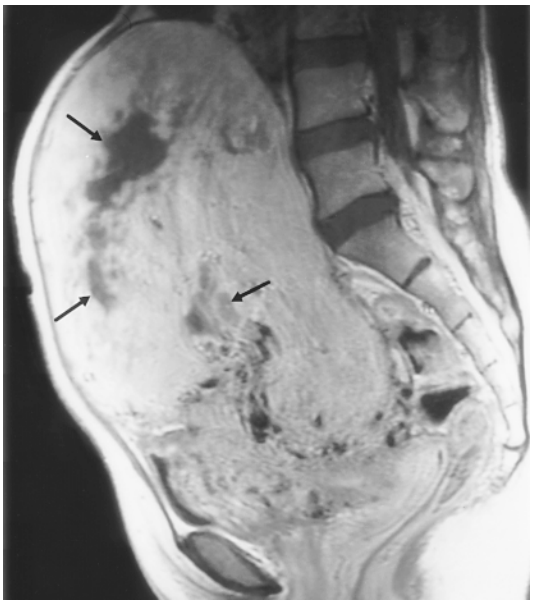

c.

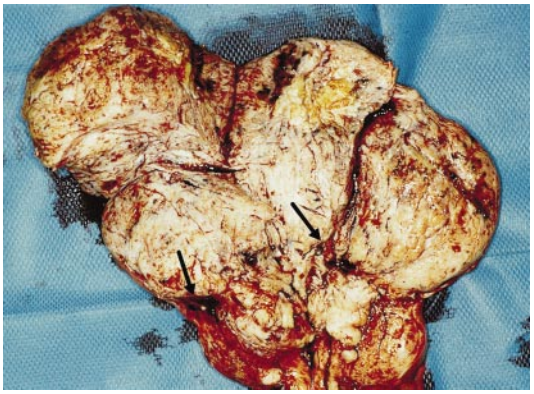

d.

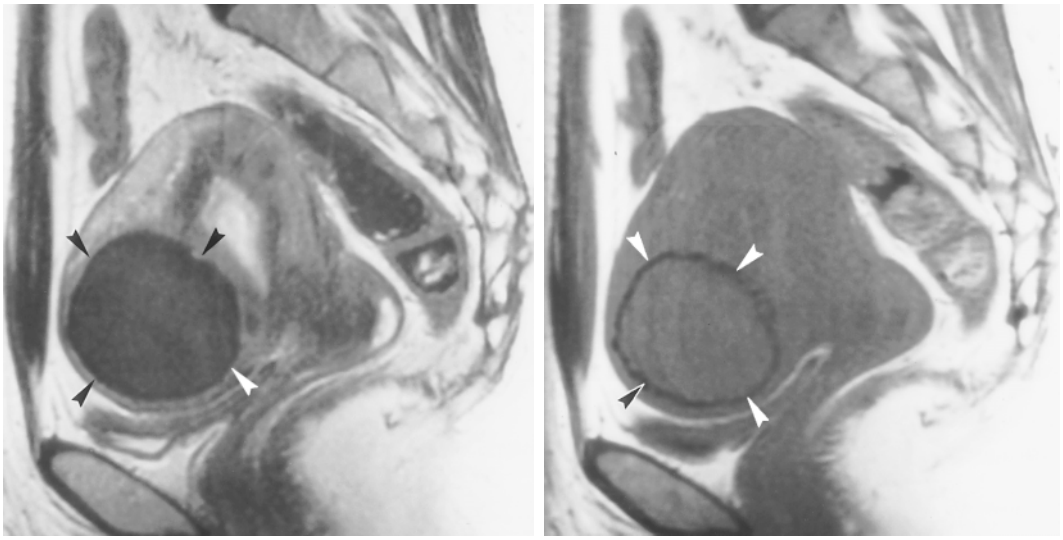

a. b.

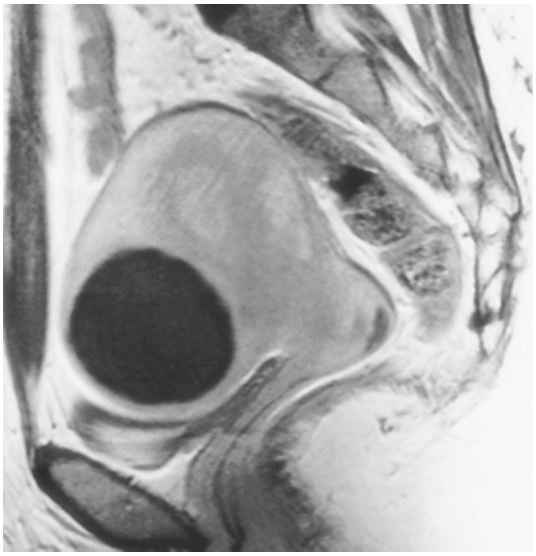

c.

Figure 8. Leiomyoma with ring calcification (probably a sequela of red degeneration) in a 42-year-old woman. The patient had experienced acute abdominal symptoms during her last pregnancy, which were indicative of red degeneration. **(a, b)** Sagittal fast spin-echo T2-weighted (6,000/126) **(a)** and spin-echo T1-weighted (600/9) **(b)** MR images show a mass with a distinct rim of low signal intensity (arrowheads). **(c)** Gadolinium-enhanced spin-echo T1-weighted MR image (600/9) shows complete absence of enhancement.

• Calcification

Secondary calcification occurs in hyalinized tissue in about 4% of leiomyomas (1). The calcification is usually dense and amorphous. This pattern of calcification at plain radiography almost exclusively indicates the diagnosis of leiomyoma. A rarely observed pattern is ringlike calcification at the margins of a leiomyoma (Fig 8). This type of calcification appears to represent thrombosed veins from past red degeneration.

■ SPECIFIC TYPES OF UNUSUAL LEIOMYOMAS

There are specific types of unusual uterine leiomyomas. These include lipoleiomyoma, myxoid leiomyoma, intravenous leiomyomatosis, metastasizing leiomyoma, diffuse leiomyomatosis, and peritoneal disseminated leiomyomatosis (1,2). The first two types may have MR imaging findings characteristic enough to allow diagnosis and are discussed in this section. The other four types represent unusual growth patterns and are discussed in the next section.

• Lipoleiomyoma

Lipoleiomyoma is a specific type of leiomyoma that contains a substantial amount of fat. The reported prevalence of lipoleiomyoma is 0.8%

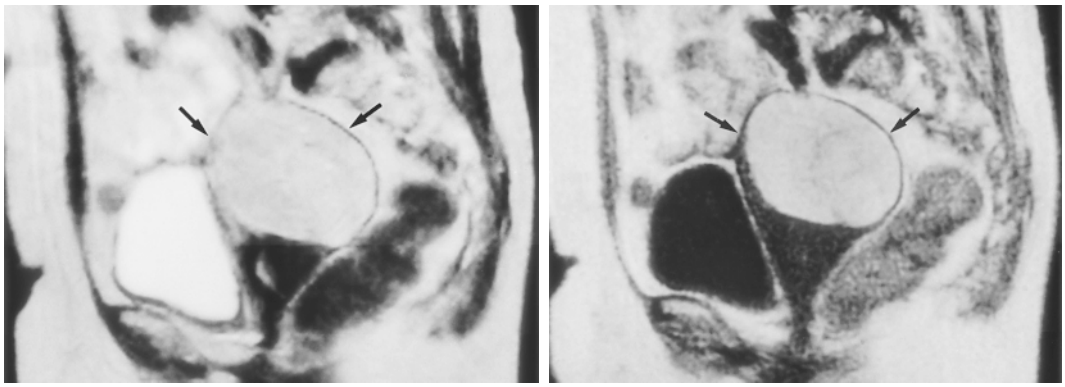

a. b.

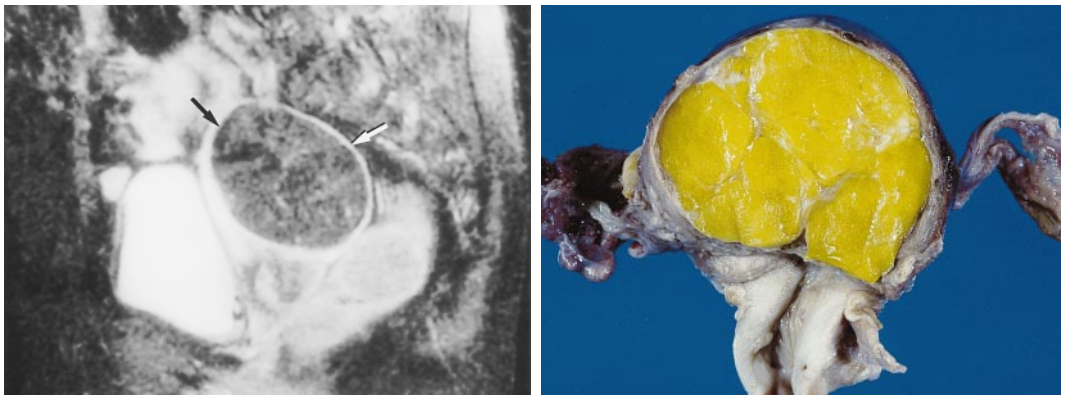

c. d.

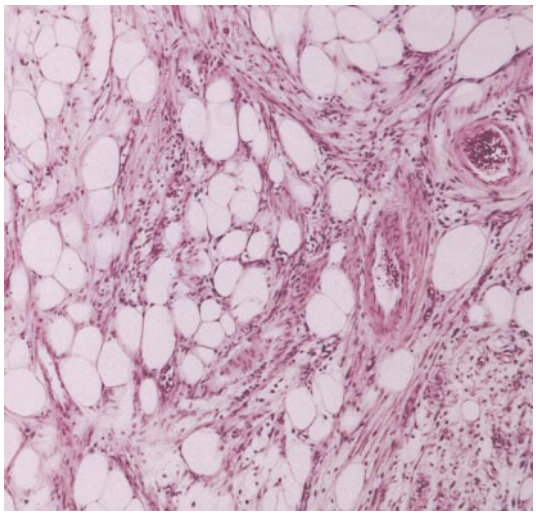

e.

Figure 9. Lipoleiomyoma in a 76-year-old woman. **(a–c)** Sagittal fast spin-echo T2-weighted (3,000/120) **(a)** and spin-echo T1-weighted (400/25) **(b)** MR images and gadolinium-enhanced spin-echo T1-weighted MR image (400/25) obtained with fat suppression **(c)** show a mass (arrows) with signal intensity equal to that of subcutaneous fat. **(d)** Photograph of the cut surface of the resected lesion shows a soft, yellow mass. **(e)** Photomicrograph (original magnification, ×200; hematoxylin-eosin stain) shows numerous adipocytes in the mass. (Fig 9a–9e courtesy of Tsuyoshi Itoh, MD, Kyoto National Hospital, Kyoto, Japan.)

(14). At microscopy, circumscribed areas of adipocytes are seen within the leiomyoma. Angiolipoleiomyoma and lipoma are related lesions and are categorized according to their microscopic components. All of these lesions are considered to represent fatty metamorphosis of leiomyoma (1,5,6), although some tumors have no smooth muscle component. At MR imaging, the fatty tissue demonstrates signal intensity similar to that of subcutaneous fat with all pulse sequences (Fig 9) (15). The fat component is usually easily differentiated from hemorrhage because of the chemical shift. However, such differentiation is sometimes difficult. In these instances, chemical shift imaging is helpful in distinguishing fat from hemorrhage.

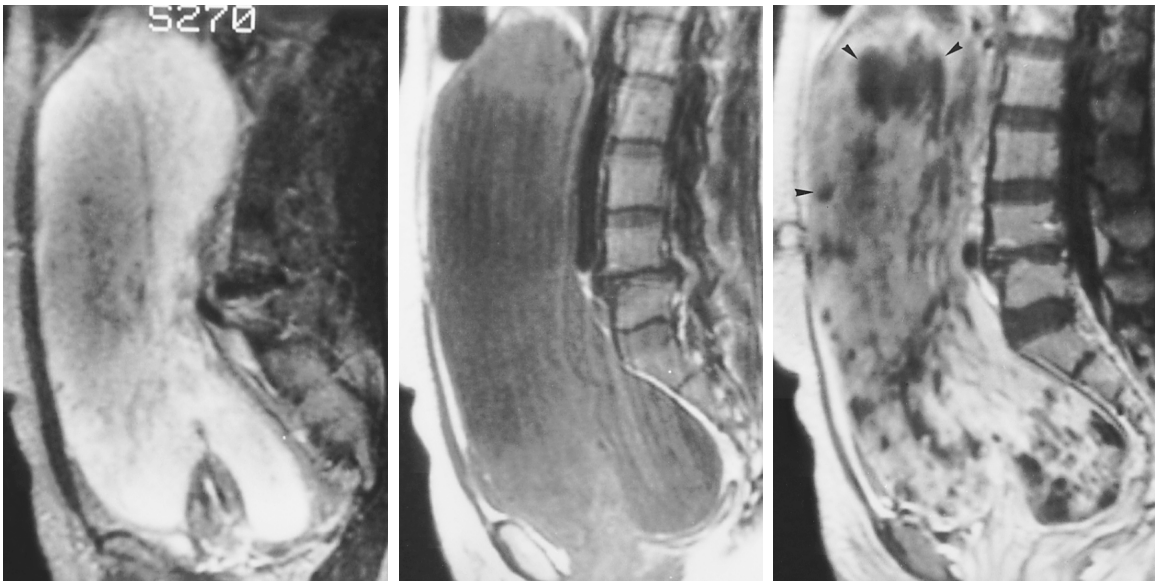

a. b. c.

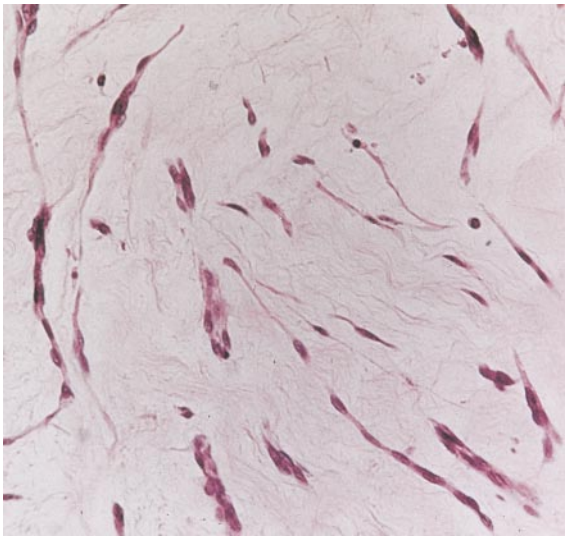

d.

Figure 10. Myxoid leiomyoma (smooth muscle tumor of uncertain malignant potential) in a 50-year-old woman. **(a, b)** Sagittal spin-echo T2-weighted (2,000/70) **(a)** and T1-weighted (600/20) **(b)** MR images show a huge mass with signal intensity similar to that of fluid: high on the T2-weighted image **(a)** and low on the T1-weighted image **(b)**. **(c)** Sagittal gadolinium-enhanced spin-echo T1-weighted MR image (600/20) shows prominent enhancement of the lesion except for small foci of mucinous lakes (arrowheads). **(d)** Photomicrograph (original magnification, ×200; hematoxylin-eosin stain) shows nuclear atypia. Smooth muscle cells are so widely separated by abundant myxoid material that mitotic count and cellularity cannot be assessed precisely.

• Myxoid Leiomyoma

Relatively rare, myxoid leiomyomas contain abundant myxoid material between smooth muscle cells. The lesions are soft and translucent but solid. Large myxoid leiomyomas may be clinically malignant even if they do not meet standard criteria for the diagnosis of sarcoma. In these lesions, smooth muscle cells are so widely separated by abundant myxoid material that mitotic count and cellularity cannot be assessed precisely (1,5,6). At MR imaging, the myxoid portion has high signal intensity on T2-weighted images and enhances well except for small foci of mucinous lakes or clefts (Fig 10). Delayed and prolonged enhancement is seen because of the presence of a myxoid stroma (16).

■ UNUSUAL GROWTH PATTERNS

Consistent with their benignity, leiomyomas have a "pushing" (instead of infiltrating) border and are rounded. However, several specific types of leiomyoma—intravenous leiomyomatosis, metastasizing leiomyoma, diffuse leiomyomatosis, and peritoneal disseminated leiomyomatosis—are exceptions to this rule. Other unusual growth patterns are retroperitoneal growth and parasitic growth. An unusual growth pattern may also occur in cervical leiomyoma.

• Intravenous Leiomyomatosis, Metastasizing Leiomyoma, Diffuse Leiomyomatosis, and Peritoneal Disseminated Leiomyomatosis

Otherwise morphologically unremarkable types of leiomyoma, intravenous leiomyomatosis, metastasizing leiomyoma, diffuse leiomyomatosis,

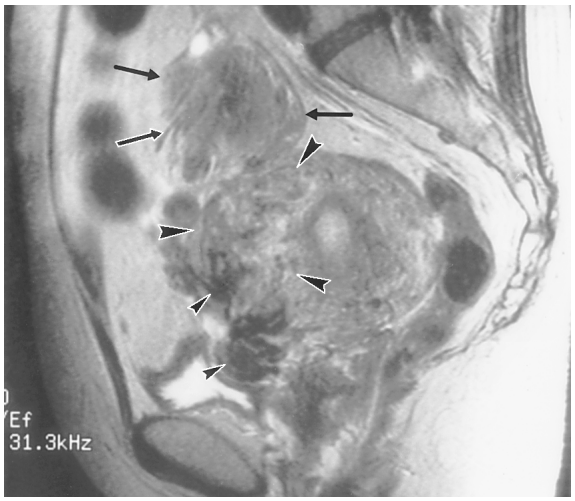

a.

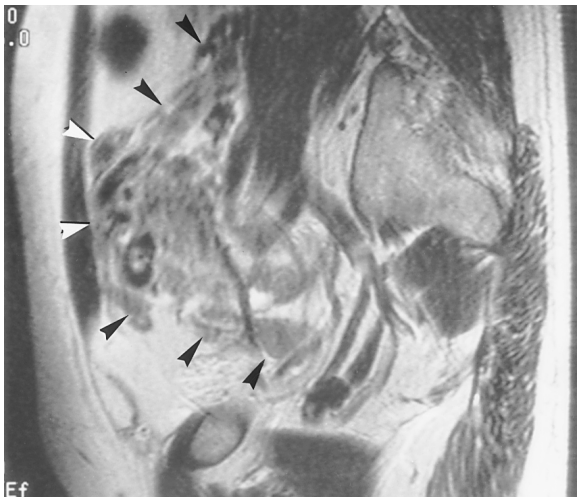

b.

Figure 11. Intravenous leiomyomatosis in a 44-year-old woman. **(a, b)** Sagittal fast spin-echo T2-weighted MR images (6,000/135) show an ill-defined, subserosal mass of low signal intensity (arrows in **a**) with multiple wormlike projections that extensively involve the myometrium, parametrium, adnexa, and gonadal veins (large arrowheads in **a**, arrowheads in **b**). The wormlike projections are accompanied by prominent signal voids (small arrowheads in **a**). **(c)** Photograph of the resected specimen shows the subserosal tumor (arrows) and wormlike projections (arrowheads).

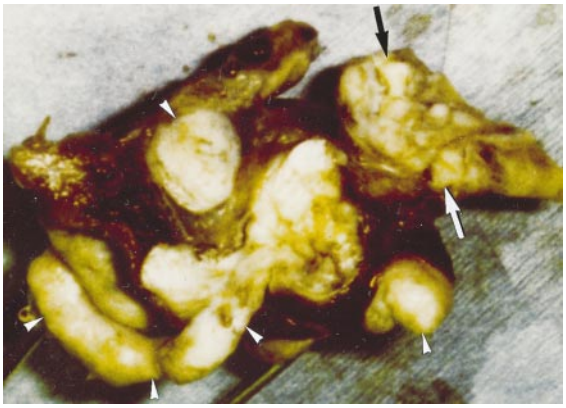

c.

and peritoneal disseminated leiomyomatosis represent only variations in growth patterns. Although histologically benign, these leiomyomas grow into veins, metastasize to distant organs, diffuse throughout the uterine parenchyma, or disseminate throughout the peritoneal cavity.

Intravenous leiomyomatosis is a rare condition characterized by growth of smooth muscle cells into the myometrial or pelvic veins. Convoluted, wormlike masses growing within the veins are the hallmark of intravenous leiomyomatosis (Fig 11) (17,18).

Benign metastasizing leiomyoma consists of smooth muscle tumors in the lungs, lymph nodes, or abdomen that appear to originate from a benign uterine leiomyoma, which typically was removed many years earlier. Because the primary tumor often has been inadequately studied, this condition is still controversial.

Diffuse leiomyomatosis involves development of innumerable small leiomyomas, which produce symmetric enlargement of the uterus. In this condition, the leiomyomas replace most of the uterine parenchyma.

Peritoneal disseminated leiomyomatosis is characterized by multiple smooth muscle nodules on the peritoneal surfaces in women of reproductive age. Only about 50 cases of peritoneal disseminated leiomyomatosis have been reported (19). It is difficult to distinguish multiple peritoneal nodules from peritoneal dissemination (20). Peritoneal disseminated leiomyomatosis is initiated or promoted by hormonal factors; the leiomyomas regress after hormonal stimulation is stopped. Many of the reported cases have been associated with pregnancy.

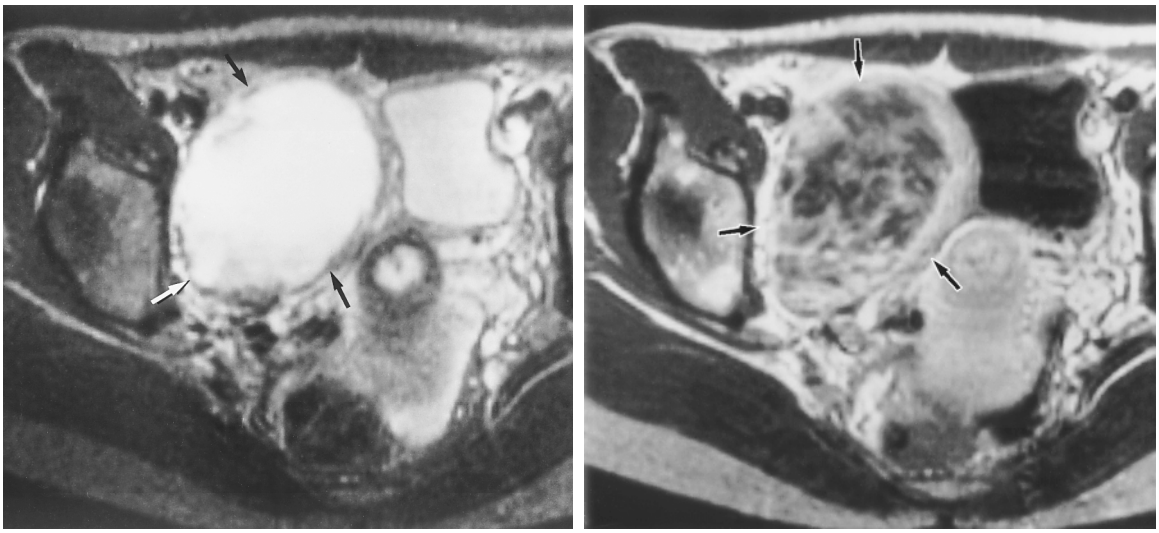

a. **b.**

Figure 13. Leiomyoma attached to the fallopian tube in a 32-year-old woman. Axial spin-echo T2-weighted (2,000/70) **(a)** and gadolinium-enhanced T1-weighted (600/20) **(b)** MR images show a mass (arrows), which demonstrates high signal intensity on the T2-weighted image **(a)** and heterogeneous enhancement on the gadolinium-enhanced image **(b)**. This myxoid leiomyoma had a blood supply only from the fallopian tube and was considered to be a parasitic growth, although this fact was not clear at MR imaging.

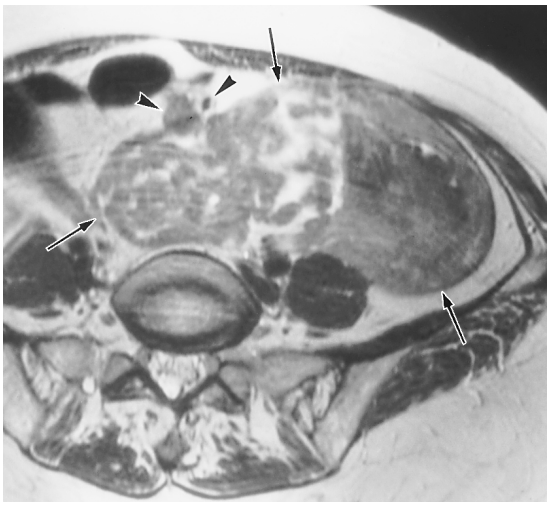

Figure 12. Leiomyoma with extensive intraligamental growth in a 55-year-old woman. Axial fast spin-echo T2-weighted MR image (6,000/86.8) shows anterior displacement of the descending colon (arrowheads) by a mass (arrows). Although the lesion appears to be a retroperitoneal tumor, surgery demonstrated a leiomyoma growing into the retroperitoneum within the broad ligament.

• Retroperitoneal Growth

Leiomyomas usually grow into the peritoneal cavity. However, they sometimes demonstrate retroperitoneal growth, usually within the broad ligament. In this situation, the leiomyoma mimics a retroperitoneal tumor by displacing the bladder, rectum, or even descending colon anteriorly (Fig 12). Because of the pressure of the surrounding tissue, the lesion tends to have an irregular rather than rounded configuration. Identification of feeding or draining vessels arising from the myometrium is helpful in distinguishing an intraligamental leiomyoma from a retroperitoneal tumor (21).

• Parasitic Growth

A pedunculated leiomyoma may lose its connection with the uterus due to torsion and necrosis of the pedicle. The leiomyoma may then become attached to other pelvic structures or the omentum and be supplied by parasitic vessels (Fig 13).

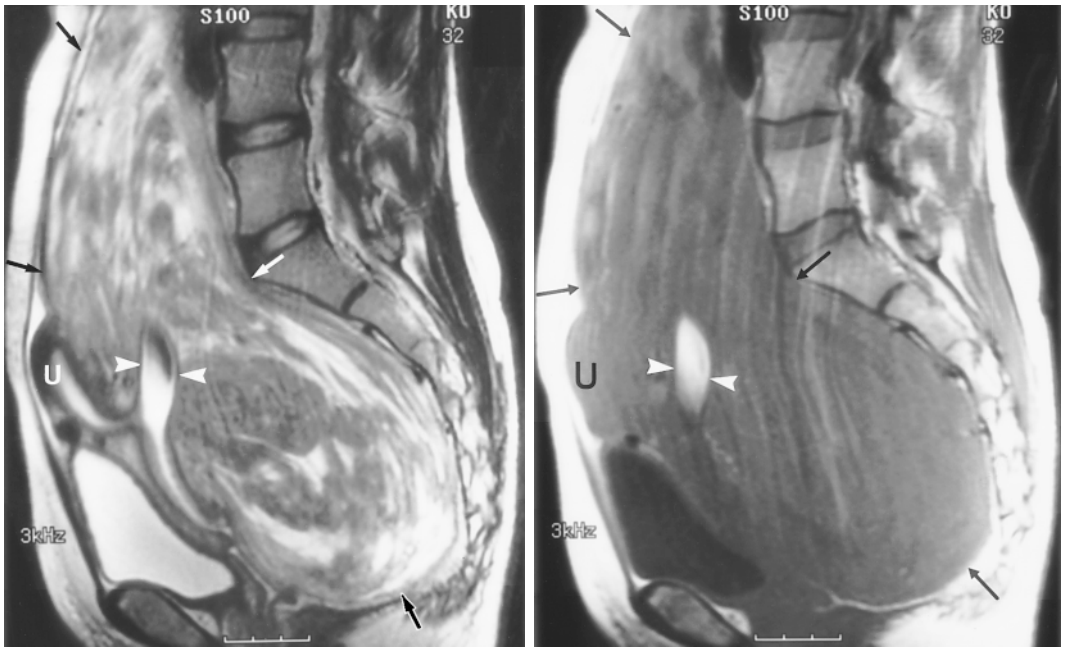

a. b.

Figure 14. Huge cervical leiomyoma in a 32-year-old woman. **(a, b)** Sagittal fast spin-echo T2-weighted (4,000/130) **(a)** and nonenhanced spin-echo T1-weighted (600/10) **(b)** MR images show a huge leiomyoma (arrows) posterior to the uterus (*U*). The cervical canal (arrowheads) is folded into the myoma. **(c)** Diagram shows the relationships between the mass (*M*), cervical canal (*), and uterus (*u*).

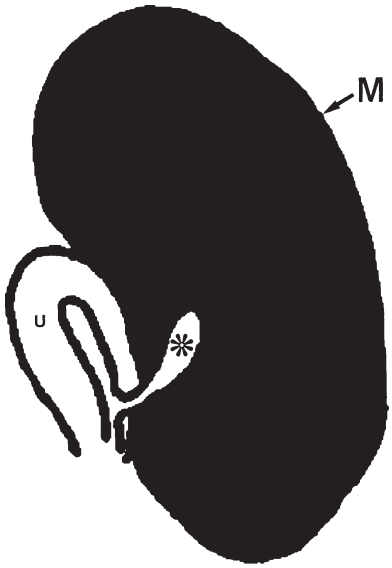

c.

● Unusual Growth Pattern in Cervical Leiomyoma

We have encountered several cases of cervical leiomyomas with an unusual growth pattern. The findings include an ill-defined rather than pushing border and incorporation of the adjacent cervical canal into the leiomyoma (Fig 14).

■ CONCLUSIONS

Uterine leiomyomas demonstrate various types of degeneration, growth patterns, clinical courses, and complications. The MR imaging appearances of leiomyomas vary widely and may present a diagnostic problem. The differential diagnosis includes a wide range of gynecologic and nongynecologic diseases. It is important to differentiate leiomyomas from other diseases because therapeutic options for leiomyomas include observation, whereas other conditions, especially malignancies, necessitate surgery. Precise knowledge of the histopathologic background and clinical courses of leiomyoma allows us to distinguish leiomyoma with an unusual appearance from gynecologic malignancies.

Acknowledgments: We thank Fumie Ametani, MD, Tsuyoshi Itoh, MD, Tadashi Sagoh, MD, Masato Noguchi, MD, and the members of the Department of Obstetrics and Gynecology, Kyoto University, for their sincere cooperation.

■ REFERENCES

1. Zaloudek C, Norris HJ. Mesenchymal tumors of the uterus. In: Kurman RJ, ed. Blaustein's pathology of the female genital tract. New York, NY: Springer-Verlag, 1994; 487–498.
2. Silverberg SG, Kurman RJ. Smooth muscle and other mesenchymal tumors. In: Rosai J, ed. Tumors of the uterine corpus and gestational trophoblastic disease, fasc 3, ser 3. Washington, DC: Armed Forces Institute of Pathology, 1992; 113–130.
3. Hricak H, Tscholakoff D, Heinrichs L, et al. Uterine leiomyomas: correlation of MR, histopathologic findings, and symptoms. Radiology 1986; 158:385–391.
4. Togashi K, Ozasa H, Konishi I, et al. Enlarged uterus: differentiation between adenomyosis and leiomyoma with MR imaging. Radiology 1989; 171:531–534.
5. Woodruff JD, Parmley TI. Atlas of gynecologic pathology. Philadelphia, Pa: Lippincott-Raven, 1988.
6. Rosai J. Ackerman's surgical pathology. 8th ed. St Louis, Mo: Mosby–Year Book, 1996; 1429–1433.
7. Ooto H, Nanbu Y, Nonogaki H, et al. Treatment with LH-RH analog, buserelin, for uterine leiomyoma: assessment with MR imaging. Endometriosis Kenkyukai Kaishi 1989; 10:245–249.
8. Oguchi O, Mori A, Kobayashi Y, Horiuchi A, Nikaido T, Fujii S. Prediction of histopathologic features and proliferative activity of uterine leiomyoma by magnetic resonance imaging prior to GnRH analogue therapy: correlation between T2-weighted images and effect of GnRH analogue. J Obstet Gynaecol 1995; 21:107–117.
9. Kawakami S, Togashi K, Konishi I, et al. Red degeneration of uterine leiomyoma: MR appearance. J Comput Assist Tomogr 1994; 18:925–928.
10. Mittl RL Jr, Yeh IT, Kressel HY. High-signal-intensity rim surrounding uterine leiomyomas on MR images: pathologic correlation. Radiology 1991; 180:81–83.
11. Okizuka H, Sugimura K, Takemori M, Obayashi C, Kitao M, Ishida T. MR detection of degenerating uterine leiomyomas. J Comput Assist Tomogr 1993; 17:760–766.
12. Kempson RL, Hendrickson MR. Pure mesenchymal neoplasms of the uterine corpus: selected problems. Semin Diagn Pathol 1988; 5:172–198.
13. Schwartz LB, Zawin M, Carcangiu ML, Lange R, McCarthy S. Does pelvic magnetic resonance imaging differentiate among the histologic subtypes of uterine leiomyomata? Fertil Steril 1998; 70:580–587.
14. Dellacha A, Di Marco A, Foglia G, Fulcheri E. Lipoleiomyoma of the uterus. Pathologica 1997; 89:737–741. [Italian]
15. Tsushima Y, Kita T, Yamamoto K. Uterine lipoleiomyoma: MRI, CT, and ultrasonographic findings. Br J Radiol 1997; 70:1068–1070.
16. Arkun R, Memis A, Akalin T, Ustun EE, Sabah D, Kandiloglu G. Liposarcoma of soft tissue: MRI findings with pathologic correlation. Skeletal Radiol 1997; 26:167–172.
17. Rotter AJ, Lundell CJ. MR of intravenous leiomyomatosis of the uterus extending into the inferior vena cava. J Comput Assist Tomogr 1991; 15:690–693.
18. Kawakami S, Sagoh T, Kumada H, et al. Intravenous leiomyomatosis of uterus: MR appearance. J Comput Assist Tomogr 1991; 15:686–689.
19. Losch A, Kainz C, Gitsch G, Breitenecker G. Disseminated peritoneal leiomyomatosis. Wien Klin Wochenschr 1996; 108:153–156. [German]
20. Papadatos D, Taourel P, Bret PM. CT of leiomyomatosis peritonealis disseminata mimicking peritoneal carcinomatosis. AJR 1996; 167:475–476.
21. Torashima M, Yamashita Y, Matsuno Y, et al. The value of detection of flow voids between the uterus and the leiomyoma with MRI. JMRI 1998; 8:427–431.